

Coulomb drag effect in parallel quantum dots

B. Tanatar* and V. Moldoveanu†

**Department of Physics, Bilkent University, Bilkent, 06800 Ankara, Turkey*

†*National Institute of Materials Physics, P.O. Box MG-7, 077125 Bucharest-Magurele, Romania*

Abstract. We study theoretically the electronic transport in parallel few-level quantum dots in the presence of both intradot and interdot long-range Coulomb interaction. Each dot is connected to two leads and the steady-state currents are calculated within the Keldysh formalism using the random-phase approximation for the interacting Green functions. Due to the momentum transfer mechanism between the two systems it is possible to get a nonvanishing current through an unbiased Coulomb-blockaded dot if the other dot is set in the nonlinear transport regime. The transitions between the levels of the passive dot reduce the drag current and lead to negative differential conductance.

Keywords: Coulomb drag effect, Quantum dots, Nanoelectronic devices

PACS: 73.23.-b, 73.63.-b, 73.21.La, 85.35.-p

INTRODUCTION

More than a decade ago Gramila *et al.* [1] measured for the first time a finite current through an unbiased two-dimensional semiconductor layer when a current passes a nearby identical layer. Nowadays it is generally accepted that the mechanism behind the observed drag current is the inelastic Coulomb scattering. [2] The electrons exchange momentum during these scattering processes and this induces a voltage drop in the passive layer, henceforth a current appears. In the standard Coulomb drag the induced current flows in the same direction as the one in the driven subsystem. Later on other experiments were performed with one-dimensional quantum wires (see [3, 4] and references therein) and even a negative Coulomb drag was reported. [5]

On the other hand a different class of experiments with Coulomb-coupled mesoscopic interferometers show that the resonant tunneling through a quantum dot can be recorded by a so-called charge detector and, conversely, the latter scrambles the coherence properties via measurement-induced dephasing. [6] Other experiments considered speculate the charge sensing effect in quantum point contacts [7] in order to extract time-resolved tunneling in quantum dots. [8] More recently, McClure *et al.* [9] reported on the current cross-correlation in Coulomb-coupled quantum dots, when each dot is individually biased.

Starting from these findings one can naturally wonder if an analog Coulomb drag could appear in quantum dot systems. More precisely, the question is whether an unbiased dot coupled to two leads and set in the Coulomb blockade regime could be set to transmit when a (possibly high) bias is applied on a second nearby dot coupled to other two leads.

On the theoretical side, the Coulomb drag effect is mostly described via the linear response theory with respect to the bias applied on the drive subsystem, and the effective layer interaction is usually computed within the random-phase approximation (see e.g.

the review paper [2] and the recent paper by Asgari *et al.* [10]). As for the current correlations one could rely on scattering formalism for interacting systems [11] or on the quantum Master equation up to the second order in the tunneling Hamiltonian. [12] In the first approach one computes the first-order contribution of the Coulomb interaction to the two-particle S -matrix, which would therefore describe the charge sensing effect but misses the inelastic scattering processes responsible for the Coulomb drag. Also, the intradot interaction is neglected.

In this paper we present transport calculations for few-level Coulomb-coupled quantum dots obtained from a recently developed random-phase approximation method for the non-equilibrium Green functions. [13] The method can deal with dephasing effects and when applied to a setup similar to the one proposed by McClure *et al.* [9] it clearly supports the existence of a Coulomb drag effect in a double dot system. We also identify some specific features like negative differential conductance regime for the unbiased system due to the intradot transitions or temperature effects.

The rest of the paper is organized as follows. Section II presents the model and gives the main equations. Section III contains the numerical results and their discussion. We conclude in Section IV with a brief summary.

THE MODEL

We shall use a tight-binding Hamiltonian to describe the two subsystems. The Hamiltonians of the non-interacting quantum dots are denoted by H_i ($i = 1, 2$) and the leads are modelled as one-dimensional chains, their Hamiltonian being denoted by H_L . The lead-dot coupling H_T and the Coulomb interaction H_I are included adiabatically through a smooth switching function $\chi(t)$. The on-site energies in each quantum dot are given by $\epsilon_m^{(i)}$ and the creation/annihilation operators by $c_{m_i}^\dagger/c_{m_i}$. The index i indicates that the site m belongs to QD_i . The states in the leads are denoted by q_l where $l = L1, R1, L2, R2$. We use creation/annihilation operators $d_{q_l}^\dagger$ and d_{q_l} . Then, the Hamiltonian of the coupled system reads therefore as follows:

$$H(t) = H_1 + H_2 + H_L + \chi(t)(H_T + H_I) \quad (1)$$

where

$$H_i = \sum_{i=1}^2 \sum_{m,n \in \text{QD}_i} (\epsilon_m^{(i)} \delta_{mn} + t_{mn}^{(i)}) c_{m_i}^\dagger c_{n_i}, \quad (2)$$

$$H_T = \sum_{i,n} \sum_{l,q} (V_{n_i q_l} c_{n_i}^\dagger d_{q_l} + h.c.), \quad (3)$$

$$H_I = \sum_{i,j} \sum_{m,n} W_{0,n_i m_j} c_{n_i}^\dagger c_{n_i} c_{m_j}^\dagger c_{m_j}, \quad (4)$$

We introduced the hopping integrals $V_{n_i q_l}$ between the leads and the sample. $W_{0,n_i m_j} = U/|r_n^{(i)} - r_m^{(j)}|$ is the bare Coulomb potential depending on the constant U and on the distance between two sites from the double-dot system. By taking a nearest-neighbor

coupling between the leads and the dots and V_{n,q_l} has four non-vanishing elements $V_{L1(R1)}$ and $V_{L2(R2)}$. Also, $t_{mn}^i = t_D$ if m, n are nearest neighbors and zero otherwise. Each lead has its own chemical potential included in the corresponding Fermi functions. Within the Green-Keldysh formalism the steady-state current entering QD₁ from the left lead (t_L is the hopping energy on leads) is given by (see [13])

$$J_1 = \frac{e}{h} \int_{-2t_L}^{2t_L} dE \text{Tr} \{ \Gamma_{L1} G^R \Gamma_{R1} G^A (f_{L1} - f_{R1}) - \Gamma_{L1} G^R \text{Im}(\Sigma_I^< + 2f_{L1} \Sigma_I^R) G^A \}. \quad (5)$$

The Green functions in Eq. (5) should be computed from the Dyson equation in the Keldysh space

$$G = G_0 + G_0(\Sigma_L + \Sigma_I)G, \quad (6)$$

written in terms of the Green function of the disconnected non-interacting system G_0 . $\Sigma_{I,L}$ are the interaction self-energy and the leads' self-energy, respectively. $\Gamma_{L1} = \Gamma_{R1}$ are coupling matrices. The random-phase approximation scheme is implemented as follows. We define the contour-ordered polarization operator Π_{mn} which is used to construct the screened interaction W , with the retarded, lesser and greater components given by the Dyson and Keldysh equations:

$$W^R(E) = W_0 + W_0 \Pi^R(E) W^R(E) \quad (7)$$

$$W^{<,>}(E) = W^R(E) \Pi^{<,>}(E) W^A(E). \quad (8)$$

The numerical simulation presented in Section III were mostly performed within the non-selfconsistent scheme which takes however into account the creation of electron-hole pairs in the double dot system. The self-consistent scheme requires more computational effort because of the convergence condition. We compare the two approaches at the end of Section III and show that they lead to qualitatively similar results. The expansion of the effective interaction W with respect to W_0 leads easily to the standard form of the interaction self-energy:

$$\Sigma_I = \Sigma_H + \Sigma_X + \Sigma_C, \quad (9)$$

where the Hartree, exchange and correlation contributions have been separated. [15] Note that (i) Σ_H does not contribute to the second term in the current since it has no imaginary part; (ii) in the G_0W approximation Σ_X cannot couple sites from different dots because the noninteracting Green function has a block-diagonal form. The effect of the interdot interaction is then expected to come from higher-order diagrams containing the electron-hole bubble.

The lesser Green function can be used to compute the occupation number N_i of each dot or the density of states ρ_i (DOS), according to the definitions:

$$N_i = \frac{1}{2\pi} \sum_{m \in \text{QD}_i} \int_{-2t_L}^{2t_L} dE \text{Im} G_{mm}^< = \int_{-2t_L}^{2t_L} dE \rho_i(E) \quad (10)$$

In this work we consider only the long-range Coulomb interaction and disregard the on-site Hubbard interaction as well as the spin degree of freedom.

RESULTS

The numerical calculations we shall present below were performed for 3-site quantum dots that are coupled to one-dimensional leads. The hopping constant on the leads is denoted by t_L and is taken as the energy unit for the bias and the interaction strength. The current is given in units of et_L/h . The first quantum dot QD₁ is coupled to unbiased leads, while the second dot is subjected to a bias $V_2 = \mu_{L2} - \mu_{R2}$. We will study the transport properties of QD₁ when the second dot is driven out of equilibrium by varying V_2 such that the bias window covers the quantum dot levels one by one. This setup corresponds more to the experiment of McClure *et al.* [9]

The passive dot is set in the Coulomb blockade regime, by taking the chemical potentials of the leads $\mu_{L1} = \mu_{R1} = \mu_0 = 1.0$; in this situation the highest level of the dot is well above μ_0 and the other two below it. The transport through the active dot is now controlled by the applied bias. The latter is varied by gradually decreasing μ_{R2} from 3 to -3 while the chemical potential of the left lead is fixed (i.e. $\mu_{L2} = 3$). Through the variation of μ_{R2} the levels of the active dot become available for transport and as a consequence we expect a Coulomb-induced response of the passive dot. Figs. 1(a) and (b) confirm that a current passing through the active dot leads to a drag current in the passive dot. Indeed, the onset of a current in QD₂ at $V_2 \sim 1.25$ corresponds to the appearance of a current in QD₁. We note that the drag current has the same sign as the driving current J_2 . This suggests that the mechanism behind the Coulomb drag in parallel double quantum dots is the same as in the bilayer systems.

One can also observe that this setup leads to a sawtooth like behavior of the dragged current rather than to a series of peaks. This is because in this situation the levels of the active dots enter the bias window one by one and remain there. Note that the dragged current however saturates when the lowest level of the active dot passes above μ_{R2} . The sawtooth like behavior is due to the fact that in some regions $dJ_1/dV_2 < 0$, that is, the differential conductance of the passive dot is negative. In order to understand this aspect analysed the occupation number N_1 as a function of V_2 . Fig. 2(a) shows that N_1 decreases when one level of QD₂ enters the bias window, but also that between two steps of J_2 the occupation number of QD₁ *increases* slightly as well, especially in the case $U = 0.1$. This means that in these regions some charge actually accumulates in the dot. This happens when the energy transferred in the inelastic scattering processes increases and matches the gaps $E_3 - E_2$, $E_2 - E_1$, or $E_3 - E_1$, $E_{1..3}$ being the levels of the passive dot. We have actually checked this fact by looking at the density of states in QD₁ (not shown). Also, if we consider only single site dots and repeat the numerical calculations of the dragged current we get a single step in J_1 and no negative differential conductance; this confirms our explanations about the competing role of the intradot transitions (no transitions are possible in the single-level case).

We remark that the drag current saturates when the lowest level of the active dot passes above μ_{R2} . The occupation number N_2 given in Fig. 2(b) confirms this scenario: N_1 decreases in step and reaches a constant value 1.5 which corresponds to half-filling of the active dot in the steady-state regime.

Fig. 3(a) shows the effect of the lead-dot coupling that characterizes the passive dot. In configuration A the relaxation processes from the level located above the chemical potential of the leads are enhanced, because the tunneling rates in and out of the dot

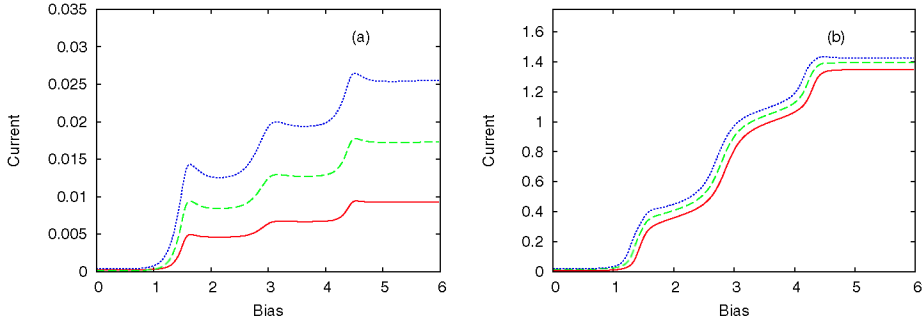


FIGURE 1. (Color online) (a) The currents through the passive dot as a function of the bias V_2 applied on the active dot for different values of the interaction strength. Full line - $U = 0.05$, dashed line - $U = 0.075$, dotted line - $U = 0.1$. (b) The current through the active dot as a function of V_2 . Other parameters: $V_{L1} = V_{R1} = 0.25$, $V_{L2} = V_{R2} = 0.5$, $kT = 0.001$.

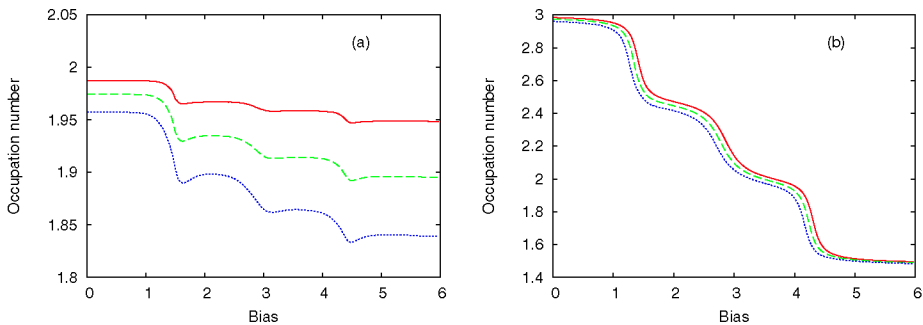


FIGURE 2. (Color online) a) The occupation number of the passive dot as a function of V_2 . (b) The occupation number N_2 as a function of the applied potential. Other parameters: $V_{L1} = V_{R1} = 0.25$, $V_{L2} = V_{R2} = 0.5$, $kT = 0.001$.

increase as the lead-dot coupling increases. Also, the electronic number within the dots is not quantized anymore and the level broadening increases. The drag effect can still be observed and at higher coupling one gets a step-like structure of the current, the regions with negative differential conductance being again washed out. Note that since the active dot is not affected when the couplings $V_{L1,R1}$ are varied the onset of the drag current appears roughly at the same value of V_2 .

As we have already mentioned, the present scheme can be improved by computing self-consistently the Green functions. We find good convergence for interaction strengths up to $U = 0.2$ and rather moderate coupling to the leads. The self-consistency condition requires a larger number of steps in the energy integrals and it is therefore time and memory consuming. We compare in Fig. 3(b) the self-consistent and non-selfconsistent currents for $U = 0.1$. We find that the self-consistent current curves are shifted with respect to the ones presented here and that the drag current tends to be larger on the first

peak. Nevertheless, the results are qualitatively similar.

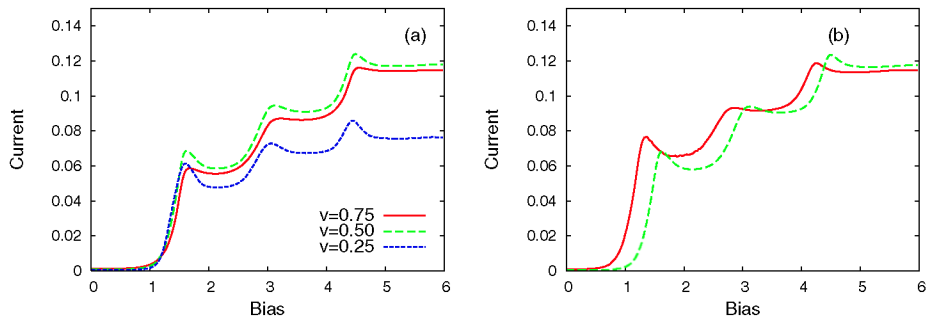


FIGURE 3. (Color online) (a) The drag current J_1 at different couplings between the passive dot and the leads. (b) Comparison between self-consistent and non-selfconsistent schemes. Full line - self-consistent result for the current through the passive dot; long-dashed line - non-selfconsistent result. Other parameters: $U = 0.1$, $kT = 0.001$, $V_{L1} = V_{R1} = 0.5$, $V_{L2} = V_{R2} = 0.5$

CONCLUSION

In this work we have investigated the Coulomb drag effect in a parallel double-quantum dot system. Each dot is coupled to two leads, one of them being set in the Coulomb blockade regime while the other is conducting due to an applied bias on the leads. Using the non-equilibrium Keldysh Green's function formalism and the random-phase approximation for the electron-electron interaction we show that a current passes through the blockaded (passive) dot when increasing the bias on the second (active) dot. The dragged current increases rather abruptly when one more level of the active dot enters the bias window. Between these jumps the passive dot also exhibits negative differential conductance (i.e. $dJ_1/dV_2 < 0$). We explain that this feature is due to the transitions between the levels of the passive dot which become possible at higher values of the driving bias and of the interaction strength. The numerical calculations given here were performed for 3-site quantum dots, but we find similar results for other configurations. We have also analysed the dependence of the Coulomb drag on the interaction strength, lead-dot coupling and temperature. In particular we have compared the selfconsistent and non-selfconsistent RPA.

ACKNOWLEDGMENTS

This work is supported by TUBITAK (No. 108T743) and TUBA. V.M. thanks the hospitality of Department of Physics, Bilkent University and acknowledges support from TUBITAK-BIDEP and Romanian Ministry of Education and Research through the PNCDI2 program.

REFERENCES

1. T. J. Gramila, J. P. -Eisenstein, A. H. MacDonald, L. N. Pfeiffer, and K. W. West, Phys. Rev. Lett. **66**, 1216 (1991).
2. A.G. Rojo, J. Phys.: Condens. Matter **11**, R31 (1999).
3. P. Debray, V. Gurevich, R. Klesse, and R.S. Newrock, Semicond. Sci. Technol. **17**, R21 (2002).
4. D. Laroche, E. S. Bielejec, J. L. Reno, G. Gervais, and M. P. Lilly, Physica E **40**, 1569 (2008).
5. M. Yamamoto, M. Stopa, Y. Tokura, Y. Hirayama, and S. Tarucha, Science **313**, 204 (2006).
6. E. Buks, R. Schuster, M. Heiblum, D. Mahalu, and V. Umansky, Nature (London) **391**, 871 (1998).
7. A.C. Johnson, C.M. Marcus, M.P. Hanson, and A.C. Gossard, Phys. Rev. Lett. **93**, 106803 (2004).
8. S. Gustavsson, R. Leturcq, B. Simovic, R. Schleser, T. Ihn, P. Studerus, K. Ensslin, D. C. Driscoll and A. C. Gossard, Phys. Rev. Lett. **96**, 076605 (2006).
9. D.T. McClure, L. DiCarlo, Y. Zhang, H.-A. Engel, C.M. Marcus, M.P. Hanson, and A.C. Gossard, Phys. Rev. Lett. **98**, 056801 (2007).
10. R. Asgari, B. Tanatar, and B. Davoudi, Phys. Rev. B **77**, 115301 (2008).
11. M.C. Goorden and M. Büttiker, Phys. Rev. B **77**, 205323 (2008); Phys. Rev. Lett. **99**, 146801 (2007).
12. S. Haupt, J. Aghassi, M.H. Hettler, and G. Schön, arXiv:0802.3579.
13. V. Moldoveanu and B. Tanatar, Phys. Rev. B **77**, 195302 (2008).
14. A.-P. Jauho and H. Smith, Phys. Rev. B **47**, 4420 (1993).
15. The explicit expression can be traced from Ref. [13]: Σ_C is given in Eqs. (21)-(24), while the exchange and Hartree contributions are given by Eq. (25) and (26).
16. V. S. Khrapai, S. Ludwig, J. P. Kotthaus, H. P. Tranitz and W. Wegscheider, Phys. Rev. Lett. **99**, 096803 (2007), Phys. Rev. Lett. **97**, 176803 (2006).